ISSN 0036-0236, Russian Journal of Inorganic Chemistry, 2019, Vol. 64, No. 12, pp. 1579–1586. © Pleiades Publishing, Ltd., 2019.
Russian Text © The Author(s), 2019, published in Zhurnal Neorganicheskoi Khimii, 2019, Vol. 64, No. 12, pp. 1326–1334.

PHYSICAL CHEMISTRY OF SOLUTIONS

Sorption of Strontium Ions on Barium Silicates from Solutions of Complex Salt Composition

P. S. Gordienko[a], I. A. Shabalin[a], S. B. Yarusova[a, b, *], S. B. Bulanova[a], V. G. Kuryavyi[a], V. V. Zheleznov[a], S. N. Somova[a], and I. G. Zhevtun[a]

[a] *Institute of Chemistry, Far Eastern Branch, Russian Academy of Sciences, Vladivostok, 690022 Russia*
[b] *Vladivostok State University of Economics and Service, Vladivostok, 690014 Russia*
**E-mail: yarusova_10@mail.ru*

Received March 29, 2019; revised May 13, 2019; accepted June 17, 2019

Abstract—The comparative analysis of sorption properties of nanostructured barium silicates obtained in multicomponent systems $BaCl_2 \cdot 2H_2O–KOH–SiO_2–H_2O$ and $BaCl_2 \cdot 2H_2O–KOH–SiO_2–AlCl_3–H_2O$ has been performed to extend previous data; the data on the composition and morphology of the systems have been presented. Their properties toward sorption of Sr^{2+} ions from solutions of complex ionic composition have been studied. It has been found that synthetic barium silicates and alumosilicates have high sorption and kinetic characteristics under static sorption conditions. The maximal degree of Sr^{2+} ions recovery from solutions of complex composition (>99%) was achieved for barium silicate $BaSiO_3 \cdot 2.3H_2O$. The samples of barium alumosilicate $BaAl_2Si_2O_8 \cdot 2.6H_2O$ have the same sorption characteristics within measurement error. It has been shown that the studied sorbents, allowing for their kinetic properties, may be recommended for the deep purification of solutions of complex ionic composition, seawater including, from strontium ions under static conditions.

Keywords: barium silicate, barium alumosilicate, sorption, strontium ions, sorption capacity, kinetics, purification extent

DOI: 10.1134/S0036023619120052

INTRODUCTION

All radioactive isotopes cause adverse effects on biogenic processes in the environment. Isotopes of such elements as strontium, cesium, cobalt, iron, etc., that have long half-life are the most dangerous isotopes to the environment. The development of nuclear power and attendant industries that provide its safe functioning and spent fuel reprocessing causes parallel works to design efficient methods and materials allowing recovery and preconcentration of radioisotopes followed by their burial or application in certain branches of industry and medicine. Radioisotope recovery from environment objects, primarily from aqueous solutions, is the urgent task. The analysis of contemporary methods for the decontamination of radionuclides from the environment shows that sorption methods are the most efficient. Research is in progress to design new sorption materials that have high selectivity of particular isotope recovery from solutions of complex ionic composition and appropriate kinetic characteristics. Efficient sorption time is of fundamental importance for sorbent application to decontaminate animals and humans.

A wide spectrum of different materials is used to recover radionuclides from aqueous media: ion-exchange resins, natural and synthetic zeolites, materials based on titanate, vanadate and tungsten, manganese oxides, ammonium hexacyanoferrates and molybdophosphates, hydroxyapatite, etc. [1–8]. Special attention of many works is focused on the use of silicates of different composition and structure and materials on their basis [9–14].

The authors [15] described a procedure for preparing nanostructured potassium alumosilicates from aqueous solutions of multicomponent systems, while the work [16] presented experimental data on the sorption properties of prepared nanostructured alumosilicates of type $K_xAl_xSi_yO_{(2y + 2x)} \cdot nH_2O$, which typically exhibit high sorption capacity toward Cs^+ ions (up to 3.7 mmol/g), high kinetic parameters under static sorption conditions (several minutes to reach 90–95% of the maximal sorption capacity), and stability under alkaline conditions.

The works [17, 18] reported the efficiency of silicates and alumosilicates for Sr^{2+} and Cs^+ recovery. Calcium alumosilicates obtained from multicomponent systems $CaCl_2–AlCl_3–KOH–SiO_2–H_2O$ with ratio Al : Si = 2 : 2, 2 : 6, and 2 : 10 were found to have sorption capacity toward strontium ions upon recovery from strontium chloride solutions without salt

background up to 0.5 mmol/g and recovery degree >90%. For modified calcium alumosilicates (in saturated calcium chloride solution) recovery degree for Sr^{2+} ions determined by radioactive-tracer technique from freshwater mimicking solutions used in the work [19] (hereafter FWM) is 90–90.5%, while $K_d = 980$, which is twice as large as ion recovery with natural alumosilicates.

The authors [20–23] reported the application of sorption reagent systems based on amorphous barium silicate $BaSiO_3$, which forms due to sol–gel transition induced by the introduction of Ba^{2+} ions in Na_2SiO_3 solution.

It was interesting to compare Sr^{2+} ions recovery from solutions of complex salt composition with barium silicate and alumosilicate prepared from aqueous solutions.

In this work, we report data on the composition, morphology, sorption properties of nanostructured barium silicates obtained in $BaCl_2 \cdot 2H_2O$–KOH–SiO_2–H_2O and $BaCl_2 \cdot 2H_2O$–KOH–SiO_2–$AlCl_3$–H_2O multicomponent systems by procedure described in [15] toward Sr^{2+} ions present in aqueous solutions of complex ionic composition.

EXPERIMENTAL

Synthesis of Barium Silicates

Barium silicate and alumosilicate was synthesized using the following chemicals: aluminum chloride $AlCl_3 \cdot 6H_2O$ and silicon dioxide $SiO_2 \cdot nH_2O$ of pure grade, potassium hydroxide of analytical grade, and barium chloride dihydrate of reagent grade.

The reactants for the synthesis of barium silicate and alumosilicate were taken in ratios corresponding to the stoichiometry of the following equations:

$$SiO_2 + 2KOH + BaCl_2 + H_2O \rightarrow BaSiO_3 + 2KCl + H_2O,$$

$$2SiO_2 + 8KOH + BaCl_2 + 2AlCl_3 + H_2O \rightarrow BaAl_2Si_2O_8 + 8KCl + 5H_2O.$$

In the synthesis of barium silicate, potassium hydroxide and silicon dioxide were dissolved in distilled water at 90–95°C and a barium chloride solution ($C = 0.1428$ mol/L) was poured into the obtained solution of potassium silicate ($SiO_2/K_2O = 1$, $C = 0.2$ mol/L) The resultant precipitate was separated by filtration and dried at 100–105°C. Barium silicate was synthesized in similar manner but subsequent keeping was carried out at 10°C for 7 days, the precipitate was separated by filtration and washed with distilled water.

Similar procedure was used to obtain barium alumosilicate. For the synthesis of barium alumosilicate, a solution of potassium silicate was added to a hot solution of barium and aluminum chlorides. The resultant precipitate was separated by filtration and washed with distilled water until negative test for chloride ions in washings.

Experiments on Sr^{2+} Ions Sorption

Strontium ions were adsorbed from aqueous solutions of strontium chloride ($SrCl_2 \cdot 6H_2O$) without salt background with Sr^{2+} ions concentration of 43.4 mg/L; from FWM solutions [19] containing the following elements (mg/L): Sr^{2+}(10–12), Ca^{2+} (100), Mg^{2+} (75), Na^+(132), K^+ (15), Cl^- (82), SO_4^{2-} (650) at solution pH 7.6; and from seawater with elemental composition (mg/L): Al (0.31), Ca (339.5), Mg (> 1000), Fe (0.07), Ba (0.02), Cd (0.04), Co (< 0.05), Cr (0.03), Cu (< 0.01), Mn (0.02), Pb (0.05), Sr (6.28), Zn (0.05).

To obtain FWM, we used potassium sulfate K_2SO_4 of high purity grade, sodium sulfate Na_2SO_4 of high purity grade, magnesium sulfate $MgSO_4 \cdot 7H_2O$ of analytical grade, calcium chloride $CaCl_2$ of reagent grade, and strontium chloride $SrCl_2 \cdot 6H_2O$ of reagent grade.

Sorption experiments were conducted under static conditions at 20°C for 3 h. Weighed samples of the studied sorbents were placed in a series of test tubes, the above solutions containing Sr^{2+} ions were added, and the mixtures were stirred on a IKA WERKE RT 15 Power magnetic stirrer (Germany). Next, the solutions were separated from the sorbent by filtration ("blue ribbon" filter paper) and concentration of Sr^{2+}, Ca^{2+}, and Ba^{2+} ions was determined.

Analysis Methods

X-ray diffraction patterns of precipitates were obtained on a ADVANCE D8 automated diffractometer (Germany) with sample spinning in CuK_α radiation. X-ray powder diffraction was carried out using EVA search program with PDF-2 powder database.

The presence of crystal water in the silicate was determined from the difference in sample weight on heating (until constant weight) up to 110 and 900°C and monitored by IR spectroscopy in the range 3000–4000 cm^{-1}.

Specific surface area of the samples was determined by low-temperature nitrogen sorption using a Sorbtometr-M device (Russia).

IR spectra were recorded in the range 400–4000 cm^{-1} on a Shimadzu FTIR Prestige-21 spectrometer (Japan) at ambient temperature. The samples for recording were grinded in an agate mortar until finely divided state and applied as Nujol mulls on a KRS-5 glass support.

To determine elemental composition of the obtained samples, we employed energy dispersive method using a Shimadzu EDX-800HS spectrometer

(Japan). The analysis was performed with no allowance for light elements using spectrometer software.

Morphology and elemental composition of the samples were determined on a Hitachi S5500 high-resolution scanning electron microscope (Japan) with add-on unit for energy dispersive analysis.

Solution pH was measured on a Multitest IPL-102 pH meter/ionometer with an ESK-10601/7 glass electrode calibrated using buffer solutions.

Chemical elements were determined in seawater by inductively coupled plasma–atomic emission spectroscopy on a Thermo Electron Scientific iCAP 6500 Duo atomic emission spectrometer (USA). Seawater was taken from the Sea of Japan in the water area of the Amur Bay (Vladivostok) and preliminary filtered using a "white ribbon" filter paper.

The content of Sr^{2+}, Ca^{2+}, and Ba^{2+} ions in the initial solutions and filtrates after sorption was determined by atomic absorption spectrometry on a Thermo Scientific SOLAAR M6 double beam spectrometer using analytical lines of 460.7, 422.6, and 553.6 nm, respectively. Determination limit in aqueous solutions is 0.002 μg/mL for strontium ions, 0.0005 μg/mL for calcium, and 0.01 μg/mL for barium. Determination error for strontium in solutions within concentration range 0.001–10 mg/L is 20%; that for calcium at concentration 0.1 through 50 mg/L is 10%; that for barium at concentration 0.01–0.2 mg/L is 30%.

The sorption capacity (A_c, mmol/g) of the studied samples was calculated by the formula:

$$A_c = \frac{(C_{init} - C_{eq})}{m}V, \quad (1)$$

where C_{init} is initial concentration of Sr^{2+} ions in solution, mmol/L; C_{eq} is equilibrium concentration of Sr^{2+} ions in solution, mmol/L; V is solution volume, L; m is sorbent weight, g.

The recovery degree of Sr^{2+} ions (α, %) was calculated by the formula:

$$\alpha = \frac{(C_{init} - C_{eq})}{C_{init}} \times 100\%. \quad (2)$$

Partition coefficient (K_d, mL/g) was determined as follows:

$$K_d = \frac{(C_{init} - C_{eq})V}{C_{eq}m}. \quad (3)$$

Strontium sorption from FWM solutions was determined by radioactive-tracer technique. Activity of solutions containing ^{90}Sr was 3×10^4 Bq/L. Purification degree was determined from the difference of ^{90}Sr concentrations in solution before and after sorption. Radionuclide content in solution was determined by β-spectrometry using a TRI-CARB model 2910 TR liquid scintillation spectrometer (Germany). Knowing

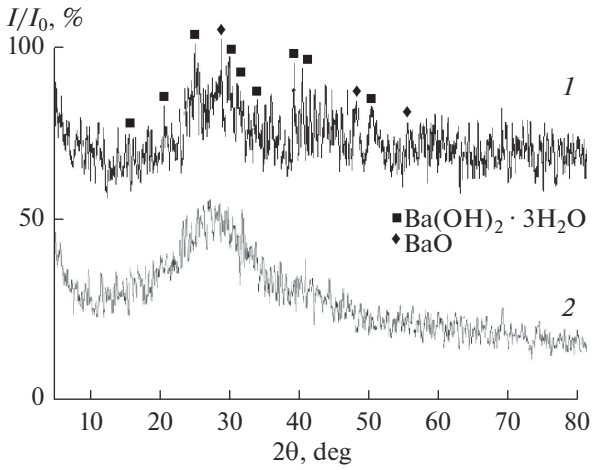

Fig. 1. Diffraction patterns for samples: (*1*) $BaSiO_3 \cdot 2.3H_2O$, (*2*) $BaAl_2Si_2O_8 \cdot 2.6H_2O$.

V/m ratio, we calculated partition coefficient based on radionuclide distribution between solid and liquid phases:

$$K_d = \left(\frac{A_s}{A_l}\right)\left(\frac{V}{m}\right), \quad (4)$$

where A_s and A_l is the content of radionuclide in solid and liquid phases, respectively. V is liquid phase volume, mL; m is sorbent weight, g.

RESULTS AND DISCUSSION

Barium Silicate Characterization

According to XRD data, the composition of the obtained samples is characterized by the presence of X-ray amorphous phases (Fig. 1), which is confirmed by registration of halo in the angle range 20°–35°.

The X-ray diffraction pattern of barium silicate sample shows two weak peaks on the background of halo corresponding to interplane distances d = 3.62614 and 3.16653 Å, which, according to database, may be related to barium hydroxide $Ba(OH)_2 \cdot 3H_2O$ and barium oxide, respectively, but it is the most probable that the samples of amorphous silicates obtained from aqueous systems contain barium carbonate, which has low solubility product value (4×10^{-10}).

The content of crystal water in the obtained samples (per mole of anhydrous silicate) is ~2.3 mol for $BaSiO_3$ and 2.6 mol for $BaAl_2Si_2O_8$. According to X-ray fluorescent analysis, the samples contain 90–93% of the noted compounds. Thus, the obtained data indicate that the composition of the synthesized samples correspond to the formulas $BaSiO_3 \cdot 2.3H_2O$ and $BaAl_2Si_2O_8 \cdot 2.6H_2O$. The values of specific surface area are 37.2 m^2/g for $BaSiO_3 \cdot 2.3\ H_2O$ and 125.3 m^2/g for $BaAl_2Si_2O_8 \cdot 2.6H_2O$.

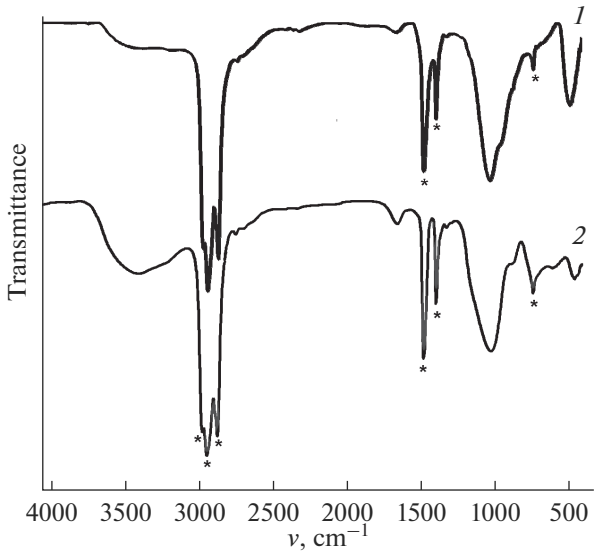

Fig. 2. IR spectra of samples: (*1*) $BaSiO_3 \cdot 2.3H_2O$, (*2*) $BaAl_2Si_2O_8 \cdot 2.6H_2O$ (* Nujol peaks).

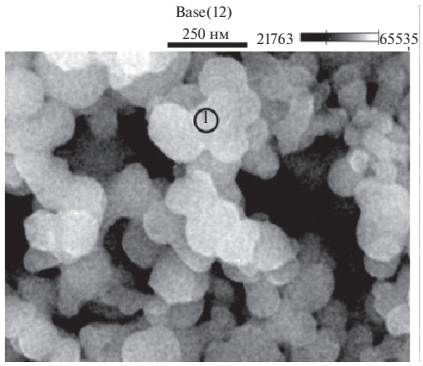

Элемент / Линия	Содержание, мас. %	Ошибка, мас. %	Содержание, ат. %	Ошибка, ат. %	Состав, мас. %
C K	28.15	+/–1.20	46.38	+/–1.96	28.15
O K	35.14	+/–1.01	43.46	+/–1.25	35.14
Si K	8.70	+/–0.30	6.13	+/–0.21	8.70
Si L	---	---	---	---	---
Ba M	---	---	---	---	---
Ba L	28.01	+/–2.14	4.04	+/–0.31	28.01
	---		---		---
Всего	100.00		100.00		100.00

Fig. 3. The SEM image, energodispersive spectrum, and elemental composition of $BaSiO_3 \cdot 2.3H_2O$ sample.

Figure 2 shows the IR spectra of barium silicate and alumosilicate samples.

The figure shows that the peak maxima of stretching and deformation vibrations of Si–O bonds of barium silicate are shifted as compared with barium alumosilicate to higher frequencies (stretching vibration frequencies are 1014.56 and 1008.77 cm^{-1} for barium silicate and alumosilicate, respectively). This is one of characteristics that confirms the enhanced energy of crystal lattice of barium silicate as compared with barium alumosilicate. In the IR spectrum of barium alumosilicate, the maximum of stretching vibration frequencies typical for crystal water (3383.14 cm^{-1}) is shifted to higher frequencies as compared with barium silicate (3118.9 cm^{-1}). This is caused by decrease of binding energy for water molecules with crystal lattice of alumosilicate.

Figure 3 exhibits the SEM image of $BaSiO_3 \cdot 2.3 H_2O$ sample and the data on barium and silicon element ratio in the local point of nanodispersed barium silicate.

The figure shows that the obtained samples of barium silicate are a powder that consists of nanodispersed spherical particles of almost the same size (diameter is not larger 50 nm). The nanoparticles produce conglomerates to give a porous system (Fig. 4).

Figure 4 shows the SEM images of barium silicate particles after keeping reaction mixture at 10°C for 7 days followed by the separation of precipitate by filtration and washing with distilled water.

Figure 4 exhibits that sample morphology is characterized by the larger content of aggregated particles, while the particles contain nanopores (Fig. 5) with diameter not larger than several Angstrom units. The nanoparticles of barium silicate sample obtained at decreased temperature (Fig. 5) are "perforated", which seems to be due to formation of nanochannels.

Barium alumosilicate (Fig. 6) consists of smaller nanoparticles, not larger than several nanometers.

Elemental ratio of barium, aluminum, and silicon in an isolated domain of barium alumosilicate sample within measurement error corresponds to the composition prescribed by the synthesis (Fig. 6).

Table 1 displays the values of partition coefficients K_d upon the sorption of Sr^{2+} ions from solutions without salt background at Sr^{2+} ions concentration of 43.4 mg/L at different ratios of solid and liquid phases (s : l).

Table 1 shows that the highest K_d values for Sr^{2+} ions sorption from solutions without salt background are typical for barium alumosilicate at all used s : l ratios.

In the study of sorption properties of barium silicate $BaSiO_3 \cdot 2.3H_2O$ samples toward Sr^{2+} ions, we found that the value of purification degree α of FWM solution with initial concentration of Sr^{2+} ions of 12 mg/L at s : l = 1 : 40, 1 : 400, and 1 : 1000 is 96.0, 88.0, and 84.0%, respectively.

At ratio s : l = 1 : 40, we calculated the value of selectivity coefficient of Sr^{2+} ions recovery relative to calcium ions $S = K_{ds}/K_{dc}$, which equals to 7. At s : l = 1 : 100, recovery degree for Sr^{2+} ions is 94.3%, while K_d = 1640. At s : l = 1 : 1000, K_d value sharply increases to 2770, while recovery degree decreases by 20.0% to reach 73.6%.

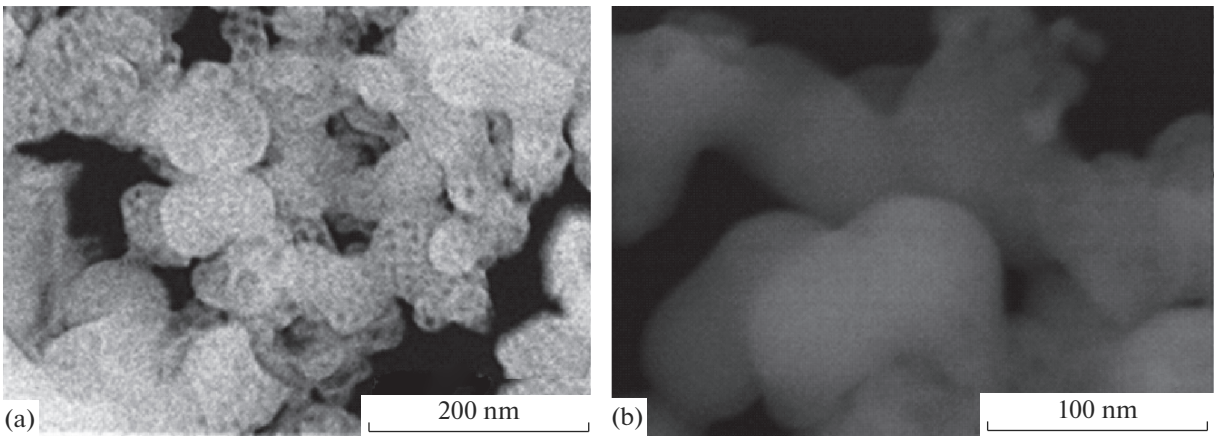

Fig. 4. The SEM image of $BaSiO_3$ after keeping reaction mixture at 10°C for 7 days.

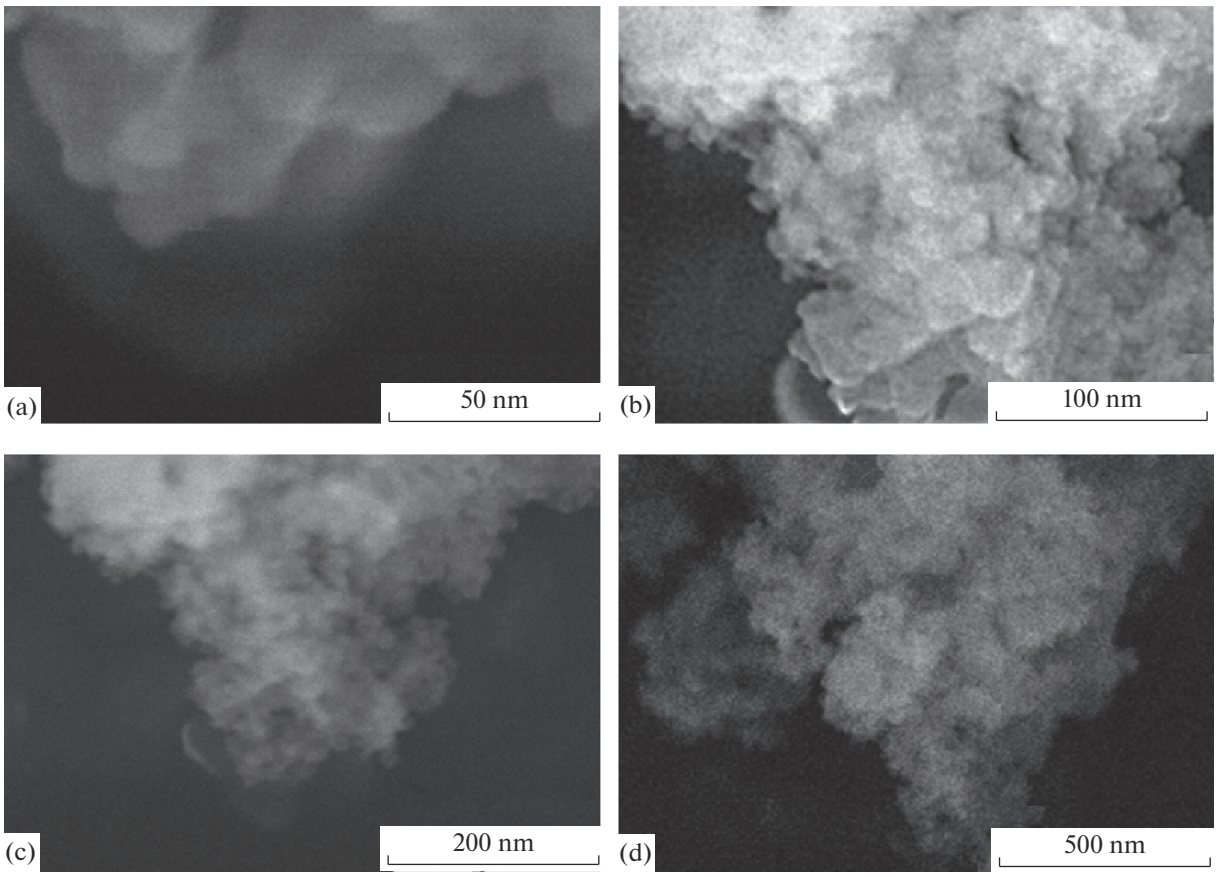

Fig. 5. The SEM image of particles of $BaAl_2Si_2O_8 \cdot 2.6H_2O$ sample.

For Sr^{2+} ions recovery from seawater with Sr^{2+} ions concentration of 6.28 mg/L at s : l = 1 : 40; 1 : 400, and 1 : 1000 (solution pH is 7.6, 8.4, and 8.3, respectively), the recovery degree of Sr^{2+} ions is within 88.0–93.0%. Using radioactive-tracer technique and ultrafiltration, we obtained data on Sr^{2+} ions recovery with barium silicate from seawater at Sr^{2+} ions concentration of 6.28 mg/L at s : l = 1 : 1000 (solution pH is 8.31). It was found that recovery degree for barium silicate >99.0%, while partition coefficient for strontium ions K_d is 0.8×10^5.

For barium alumosilicate $BaAl_2Si_2O_8$ at s : l = 1 : 40, 1 : 400, and 1 : 1000 (pH 8.15, 8.54, and 8.81, respectively), the degree of Sr^{2+} ions recovery from

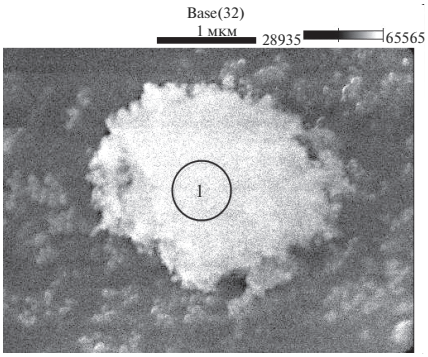

Элемент / Линия	Содержание, мас. %	Ошибка, мас. %	Содержание, ат. %	Ошибка, ат. %	Состав, мас. %
C K	18.58	+/–1.89	35.21	+/–3.63	18.56
O K	26.65	+/–0.94	37.92	+/–1.33	26.65
Al K	10.33	+/–0.49	8.71	+/–0.41	10.33
Si K	---	---	---	---	---
Si L	14.05	+/–0.59	11.39	+/–0.48	14.05
K L	---	---	---	---	---
K K	4.16	+/–0.59	2.42	+/–0.34	4.16
Ba L	26.23	+/–2.93	4.35	+/–0.49	26.23
Ba M	---	---	---	---	---
	---		---		---
Всего	100.00		100.00		100.00

Fig. 6. The SEM image and elemental composition of $BaAl_2Si_2O_8 \cdot 2.6H_2O$ sample.

FWM solution with initial Sr^{2+} ions concentration of 12 mg/L is 99.0, 98.0, and 87.0%, respectively. Partition coefficient K_d = 3880, 1593, and 6480, respectively, which is considerably higher than for natural silicate sorbents used for purification of such solutions [19].

In seawater at Sr^{2+} ions concentration of 6.28 mg/mL at s : l = 1 : 40; 1 : 400, and 1 : 1000 (solution pH is 7.6, 8.4, and 8.3, respectively), the recovery degree of Sr^{2+} ions is 97.0, 83.0, and 57.0%, respectively.

No Ba^{2+} ions were detected after sorption in the studied seawater solutions by atomic-absorption spectrometry. This is explained by the fact that both strontium silicate and barium sulfate (in the presence of sulfate ions in solution) resulting from the cation exchange of Ba^{2+} ions by Sr^{2+} ions from solutions have

Table 1. Partition coefficients for Sr^{2+} ions sorption from solutions without salt background

Compound	Ratio s : l	K_d, mL/g	Recovery degree α, %
$BaAl_2Si_2O_8 \cdot 2.6H_2O$	1 : 400	1.3×10^3	76.0
	1 : 1000	1.7×10^3	64.0
	1 : 2000	1.8×10^3	46.0
$BaSiO_3 \cdot 2.3H_2O$	1 : 400	0.6×10^3	61.0
	1 : 1000	1.1×10^3	55.0
	1 : 2000	0.7×10^3	28.0

low solubility product values (SP): 1×10^{-13} for $SrSiO_3$, 1.1×10^{-10} for $BaSO_4$, 3.98×10^{-11} for $BaSiO_3$ and therefore these compounds precipitate.

We revealed no difference in the sorption parameters of barium silicate samples obtained by mixing solutions of potassium silicate and barium chloride at 100 and 10°C followed by keeping at 10°C for 7 days in spite of marked morphological difference in powder nanotexture (Figs. 3 and 4).

Table 2 shows the data on the sorption kinetics of Sr^{2+} ions with barium silicate $BaSiO_3 \cdot 2.3H_2O$ from FWM solutions.

Empirical equation (I) which is formally reminiscent to Langmuir equation was proposed for kinetic data treatment [24]:

$$\alpha_t = \alpha_m kt\left[\frac{1}{(1+tk)}\right], \quad (5)$$

where α_m is the maximal recovery degree of the corresponding ion; t is sorption time, h; k is the constant equal to inverse sorption time for which recovery degree of determined ion reaches $1/2\alpha_m$, dimension is h^{-1}.

The value of k was calculated from the tabular data for α_t, α_m, and t values by the equation:

$$k = \alpha_t/(\alpha_m - \alpha_t)t. \quad (6)$$

On the sorption of ions from FWM solutions with barium silicate, k value equals to 140 h^{-1} for Sr^{2+} and 25 h^{-1} for Ca^{2+}. Table 1 parenthetically presents calculated by equation (1) recovery degree values for Sr^{2+} and Ca^{2+} ions.

The data of Table 2 show that the experimental and calculated values of α at the noted coefficients k differ by value Δ, %, given in Table 1. The relative difference in α_t values toward experimental data is not larger than several percent, the deviation of experimental data from that theoretically obtained by equation (5) is observed in both positive and negative side. The calculated data show that the obtained nanostructured sorbent reaches the half of the maximal sorption capacity toward strontium ions over time not longer than 30 s.

Experimental data on ion sorption kinetics were treated using the equation of pseudo-second-order kinetics [25]:

$$\frac{dA_t}{dt} = k_2(A_e - A_t)^2, \quad (7)$$

where A_t is the current value of ions recovery degree (in arb. units); A_e is the maximal value of ions recovery degree (in arb. units); k_2 is the rate constant of pseudo-second-order reaction (h^{-1}); t is sorption time (h).

Equation (7) is reduced to the form:

$$1/A_t = 1/A_e - 1/(k_2A_e^2t). \quad (8)$$

The time dependences of Ca^{2+} and Sr^{2+} ions recovery according to equation (1) are presented in Fig. 7

Table 2. Data on kinetics of $Sr^{2+}$and Ca^{2+} ions sorption on barium silicate $BaSiO_3 \cdot 2.3H_2O$ from solutions mimicking the water of influent lake no. 11, Mayak Production Association, (ratio s : l = 1 : 40 at 20°C); α_t, %, is the experimental and calculated (in parentheses) value of recovery degree for the corresponding ion; Δ, %, is the relative difference in α_t values

Parameter	*t*, h					
	0.083	0.333	0.5	0.666	1.0	1.5
α_t, % (Sr)	87.5 (87.28)	92.2 (92.80)	96.2 (93.46)	94.3 (93.79)	94.3 (94.12)	94.8 (94.35)
Δ, %	0.24	−0.6	1.3	−5.0	1.72	0.47
α_t, % (Ca)	59.7 (59.98)	86.7 (79.36)	81.4 (82.31)	84.0 (83.86)	83.3 (85.48)	88.9 (86.59)
Δ, %	−0.48	8.45	−1.1	0.16	−2.6	2.59

and described by the equations $y = 0.0449x + 1.107$ and $y = 0.0072x + 1.051$, respectively, with correlation coefficients R^2 close to 1. Parameters $A_e = 0.9033$ and $k_2 = 27.3$ h^{-1} were obtained for Ca^{2+} ions, while $A_e = 0.9513$ and $k_2 = 153.6$ h^{-1} were got for Sr^{2+} ions.

Kinetics data were treated using the Kolmogoroff–Erofeev equation used for the analysis of topochemical processes:

$$\alpha = 1 - \exp(kt^n), \quad (9)$$

where α is ions recovery degree; *k* is sorption parameter related to reaction constant by relationship $k = 1/K^n$; *t* is time (h); *n* is reaction order.

The kinetics of topochemical process of Ca^{2+} and Sr^{2+} ions sorption shown in Fig. 8 is described by the equation (10) obtained after taking the double logarithm of the equation (9):

$$\ln[-\ln(1-\alpha)] = \ln k + n\ln t. \quad (10)$$

The graphical dependences (Fig. 8) indicate that the kinetics of these reactions is described by the linear equations: $y = 0.7029 + 0.2587x$ (with correlation coefficient $R^2 = 0.8638$) and $y = 1.0529 + 0.1173x$ (with correlation coefficient $R^2 = 0.9918$) for Ca^{2+} and Sr^{2+} ions, respectively.

It follows from the obtained dependences that reaction order is 0.2587 for the sorption of Ca^{2+} ions and 0.1173 for Sr^{2+} ions. These values of reaction order are typical for diffusion-controlled processes.

CONCLUSIONS

The obtained experimental data indicate that the synthetic barium silicates and alumosilicates have high sorption and kinetic characteristics under static sorption conditions with the time to reach $1/2A_m$ value within several tens of seconds.

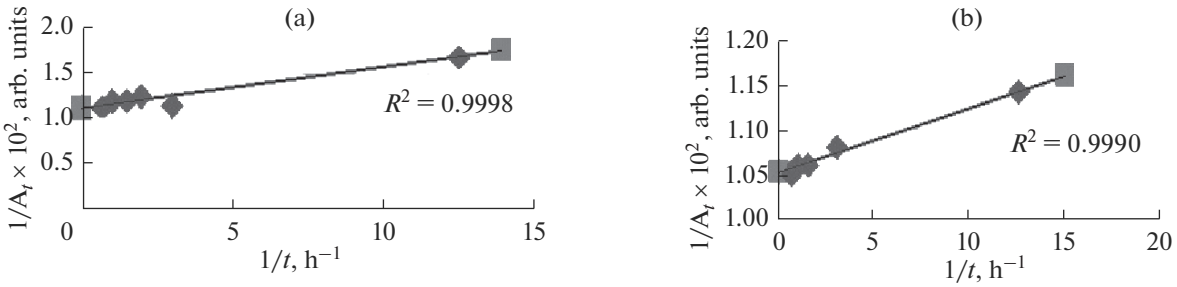

Fig. 7. Pseudo-second-order kinetic model for ion sorption: (a) Ca^{2+}, (b) Sr^{2+}.

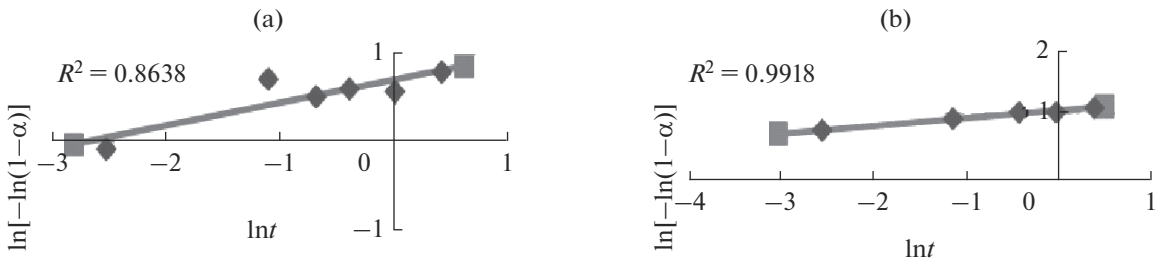

Fig. 8. Kinetics of the topochemical processes of ions sorption: (a) calcium, (b) strontium.

The maximal degree of Sr^{2+} ions recovery from solutions of complex ionic composition (>99%) was achieved for the sample of barium silicate $BaSiO_3 \cdot 2.3H_2O$. Within measurement error, the same sorption characteristics were obtained for barium alumosilicate $BaAl_2Si_2O_8 \cdot 2.6H_2O$. However, taking into account the mole fractions of barium in sorbent samples, cation exchange efficiency in barium alumosilicate is several times higher than that for barium silicate, which seems to be due to both dispersity and morphology of the obtained samples; therefore, the additional comparative study of these two types of sorbents is necessary. The difference in sorption parameter values for barium-containing sorbents should be taken into account in their synthesis and the application of such materials.

Partition coefficient for strontium ions on the use of synthetic barium silicate as a sorbent is 0.8×10^5 (at s : l = 1 : 1000), i.e., such sorbents with allowance made for their kinetic properties may be recommended for the deep purification of solutions of complex ionic composition, seawater including, from strontium ions under static conditions.

FUNDING

This work was supported by the Far East Branch of the Russian Academy of Sciences, (complex program "Dalnii Vostok", project no. 18–3–026 for 2018–2020) and the Ministry of Education and Science of the Russian Federation (State contract no. 4.5913.2017/8.9)

REFERENCES

1. D. Alby, C. Charnay, M. Heran, et al., J. Hazard. Mater. **344**, 511 (2018). https://doi.org/10.1016/j.jhazmat.2017.10.047
2. A. Merceille, E. Weinzaepfel, Y. Barre, et al., Sep. Purif. Technol. **96**, 81 (2012). https://doi.org/10.1016/j.seppur.2012.05.018
3. A. I. Ivanets, V. G. Prozorovich, T. F. Kouznetsova, et al., Environ. Nanotechnol. Monit. Manage. **6**, 261 (2016). https://doi.org/10.1016/j.enmm.2016.11.004
4. A. I. Ivanets, L. L. Katsoshvili, P. V. Krivoshapkin, et al., Radiochem. **59**, 264 (2017). https://doi.org/10.1134/S1066362217030080
5. N. V. Kitikova, A. I. Ivanets, I. L. Shashkova, et al., J. Radioanal. Nucl. Chem. **314**, 2437 (2017). https://doi.org/10.1007/s10967-017-5592-4
6. V. V. Milyutin, N. A. Nekrasova, and V. O. Kaptakov, Proc. Kola Sci. Cent. **67** (2018). https://doi.org/10.25702/KSC.2307-5252.2018.9.1.67-71
7. A. Egorin, T. Sokolnitskaya, Yu. Azarova, et al., J. Radioanal. Nucl. Chem. **317**, 243 (2018). https://doi.org/10.1007/s10967-018-5905-2
8. A. S. Portnyagin, A. M. Egorin, A. P. Golikov, et al., Thermochim. Acta **675**, 92 (2019). https://doi.org/10.1016/j.tca.2019.03.019
9. V. Montoya, B. Baeyens, M. A. Glaus, et al., Geochim. Cosmochim. Acta **223**, 1 (2018). https://doi.org/10.1016/j.gca.2017.11.027
10. J. Kim and S. -Y. Kwak, Chem. Eng. J. **313**, 975 (2017). https://doi.org/10.1016/j.cej.2016.10.143
11. R. O. Abdel Rahman, H. A. Ibrahim, M. Hanafy, et al., Chem. Eng. J. **157**, 100 (2010). https://doi.org/10.1016/j.cej.2009.10.057
12. H. Sepehrian, S. J. Ahmadi, S. Waqif-Husain, et al., J. Hazard. Mater. **176**, 252 (2010). https://doi.org/10.1016/j.jhazmat.2009.11.020
13. W. Feng, Z. Wan, J. Daniels, et al., J. Clean. Prod. **202**, 390 (2018). https://doi.org/10.1016/j.jclepro.2018.08.140
14. Y. Song, et al., J. Mol. Liq. **180**, 244 (2013). https://doi.org/10.1016/j.molliq.2013.02.003
15. RF Patent No. 2516639 (2014).
16. P. S. Gordienko, S. B. Yarusova, I. A. Shabalin, et al., Radiochem. **56**, 607 (2014). https://doi.org/10.1134/S106636221406005
17. P. S. Gordienko, I. A. Shabalin, A. P. Suponina, et al., Russ. J. Inorg. Chem. **61**, 946 (2016). https://doi.org/10.1134/S003602361608009X
18. P. S. Gordienko, I. A. Shabalin, S. B. Yarusova, et al., Russ. J. Phys. Chem. A **90**, 2022 (2016). https://doi.org/10.1134/S0036024416100125
19. O. Yu. Baranova, Protection of Water Areas from Induced Radionuclides with Sorbents Based on Opal–Cristobalite Rocks, Extended Abstract of Cand. Sci. (Eng.) Dissertation, Yekaterinburg, 2006.
20. T. A. Sokol'nitskaya, V. A. Avramenko, I. S. Burkov, et al., Zh. Fiz. Khim. **78**, 497 (2004).
21. V. A. Avramenko, I. S. Burkov, V. Yu. Glushchenko, et al., Vestn. DVO RAN, No. **3**, 7 (2002).
22. A. M. Egorin, T. A. Sokol'nitskaya, M. V. Tutov, et al., Dokl. Akad. Nauk **460** (2), 177 (2015).
23. I. G. Tananaev and V. A. Avramenko, Zh. Belorus. Gos. Univ. Ekologiya, No. **4**, 33 (2017).
24. P. S. Gordienko, I. A. Shabalin, S. B. Yarusova, et al., *Abstracts of Papers, All-Russ. Conf. on Solid-State Chemistry and Functional Materials and XII All-Russ. Symp. on Thermodynamics and Material Science,* St. Petersburg, 2018, p. 49.
25. Y. S. Ho and G. McKay, Process Biochem. **34**, 451 (1999).

Translated by I. Kudryavtsev

SPELL: OK